Received: 30 June 2023 | Revised: 30 August 2023 | Accepted: 31 August 2023

DOI: 10.1002/pamm.202300177

PAMM Proceedings in Applied Mathematics and Mechanics

RESEARCH ARTICLE

Gradient-based determination of principal design influences on composite structures

Jan Liedmann[1] | **Franz-Joseph Barthold**[1] | **Nikolai Gerzen**[2]

[1]Institute of Structural Mechanics and Dynamics, TU Dortmund University, Dortmund, Germany

[2]Department of Civil Engineering, Ostwestfalen-Lippe University of Applied Sciences, Detmold, Germany

Correspondence
Jan Liedmann, Institute of Structural Mechanics and Dynamics, TU Dortmund University, August-Schmidt-Straße 8, 44227 Dortmund, Germany.
Email: jan.liedmann@tu-dortmund.de

Funding information
Deutsche Forschungsgemeinschaft (DFG)

Abstract

This work deals with the computation of design sensitivities of elastic solid-shell structures extended to anisotropic layered composite structures. Design sensitivities concerning fiber angles and layer thicknesses are derived and quantitatively determined in the context of the finite element method. The anisotropic analysis model is founded on a sophisticated solid-shell formulation based on reduced integration and is extended to discretize the composite with only one element over the element thickness by means of multiple integration points. This can be understood as a special case of equivalent-single-layer theories. Examination of system response sensitivity matrices using methods from principal component analysis, such as singular value decomposition, is used to identify crucial design changes corresponding to major changes in the structural behavior of the composite. This procedure is termed as sensitivity based design exploration. Results are discussed by reference to simple academic examples.

1 | INTRODUCTION

Optimization of fiber-reinforced composite structures with nonlinear load-bearing behavior is a complex task that is becoming increasingly relevant in practice. Therefore, it is desirable to automatically determine essential influences on the structural behavior of fiber composite shells and stability-relevant objective functions and constraints in the context of structural optimization. These structures find widespread use in aerospace, automotive, and civil engineering industries, where optimizing their performance and reliability is of great importance. Sensitivity analysis plays a crucial role in understanding the influence of design parameters on the structural response, allowing for informed decision-making during the design process. Additionally, it enables identifying the most influential design parameters and quantify their impact on the structural performance, providing valuable insights for optimization and design improvement. In particular, this study focuses on employing singular value decomposition (SVD) as a powerful tool for extracting meaningful information from response sensitivity information. SVD is a mathematical technique widely used in various scientific and engineering disciplines for dimensionality reduction, feature extraction, and system identification, cf. for example [1]. In the context of sensitivity analysis, SVD provides a compact representation of the response sensitivity matrix by decomposing it into orthogonal modes with associated singular values. These modes capture the dominant sets of sensitivity variation, allowing for efficient exploration and interpretation of the sensitivity information in order to automate the selection of the most important design parameters. By applying SVD to the response sensitivity information of fiber reinforced composite shells, critical design parameters can be identified that have the most significant influence on the structural response. Moreover, the extracted modes and associated singular values can be utilized to rank the importance of design variables and guide the optimization process towards improved designs. The utilization of SVD in sensitivity analysis of thin-walled structures has shown promising results - especially in the context of shape optimization - in enhancing the understanding of complex structural behavior and aiding in the designing process, cf. for example [2].

In this context, utilization of sophisticated solid-shell finite elements has proven itself, cf. for example [3], and is suitable for modeling anisotropic composite behavior, as has been shown for example in [4]. The proposed modeling has the advantage that only one element has to be used in thickness direction as different layers can be easily represented by means of multiple integration points in thickness direction.

2 | STRUCTURAL ANALYSIS

Following, most important aspects of the structural analysis model used in this work are briefly sketched. First, a sophisticated solid-shell finite element proposed by [3] is reflected, followed by the extension to model anisotropic material behavior considering layered composites by means of multiple integration points along the element thickness.

2.1 | Solid-shell finite element

The solid-shell element used for structural analysis in this work has been proposed in [3]. Following, most important aspects are briefly summarized. Based on a Hu-Washizu three-field functional, the weak form of equilibrium is given by

$$\begin{aligned} R(\mathbf{u},\mathbf{X};\delta\mathbf{u}) &= \delta_u \Pi(\mathbf{u},\mathbf{X})(\delta\mathbf{u}) \\ &= \int_K \left(\delta_u \mathbf{E}(\hat{\mathbf{u}},\mathbf{X}) : \hat{\mathbf{S}} - \delta\hat{\mathbf{u}}\cdot\mathbf{b}\right)\mathrm{d}V - \int_{\partial K} \delta\hat{\mathbf{u}}\cdot\mathbf{t}\,\mathrm{d}\mathbf{A} \\ &+ \int_K \delta\hat{\mathbf{S}} : (\mathbf{E}(\hat{\mathbf{u}},\mathbf{X}) - \bar{\mathbf{E}})\,\mathrm{d}V \\ &+ \int_K \delta\bar{\mathbf{E}} : \left(\frac{\partial W(\hat{\mathbf{u}},\mathbf{X})}{\partial \mathbf{E}(\hat{\mathbf{u}},\mathbf{X})} - \hat{\mathbf{S}}\right)\mathrm{d}V = 0, \end{aligned} \tag{1}$$

where $\mathbf{u} = (\hat{\mathbf{u}}, \hat{\mathbf{S}}, \bar{\mathbf{E}})$ is the vector of state variables containing the primary unknown displacements, the assumed stresses and the assumed strains, respectively. After discretization the following system of equations has to be solved

$$\underset{e=1}{\overset{\text{nel}}{\mathsf{A}}} \begin{bmatrix} \boldsymbol{k}_e & \mathbf{0} & \mathbf{0} & \boldsymbol{L}_e^\top \\ \mathbf{0} & \boldsymbol{A}_e^{11} & \boldsymbol{A}_e^{12} & -\boldsymbol{C}_e \\ \mathbf{0} & \boldsymbol{A}_e^{21} & \boldsymbol{A}_e^{22} & \mathbf{0} \\ \boldsymbol{L}_e & -\boldsymbol{C}_e & \mathbf{0} & \mathbf{0} \end{bmatrix} \underset{e=1}{\overset{\text{nel}}{\mathsf{A}}} \begin{bmatrix} \Delta\hat{\boldsymbol{u}}_e \\ \Delta\boldsymbol{\alpha}_e^1 \\ \Delta\boldsymbol{\alpha}_e^2 \\ \Delta\boldsymbol{\beta}_e \end{bmatrix} = - \underset{e=1}{\overset{\text{nel}}{\mathsf{A}}} \begin{bmatrix} \boldsymbol{f}_e^{\text{int}} - \boldsymbol{f}_e^{\text{ext}} \\ \boldsymbol{\alpha}_e^1 \\ \boldsymbol{\alpha}_e^2 \\ \boldsymbol{b}_e \end{bmatrix}. \tag{2}$$

Static condensation on element level leads to the simplification

$$\boldsymbol{K}_e \Delta\hat{\boldsymbol{u}}_e = \boldsymbol{R}_e^{\text{ext}} - \boldsymbol{R}_e^{\text{int}}, \tag{3}$$

in which only the primary diplacements remain as unknowns. Here, the effective tangent stiffness matrix is given by

$$\boldsymbol{K}_e = \left[\boldsymbol{k}_e + \boldsymbol{L}^\top \boldsymbol{C}_e^{-1} \boldsymbol{A}_e \boldsymbol{C}_e^{-1} \boldsymbol{L}_e\right] \tag{4}$$

and the internal and external part of the residual vector are respectively given by

$$\boldsymbol{R}_e^{\text{int}} = \boldsymbol{f}_e^{\text{int}} + \boldsymbol{L}_e^\top \boldsymbol{C}_e^{-1} \left[\boldsymbol{a}_e + \boldsymbol{A}_e \boldsymbol{C}_e^{-1} \boldsymbol{b}_e\right] \quad \text{and} \quad \boldsymbol{R}_e^{\text{ext}} = \boldsymbol{f}_e^{\text{ext}}, \tag{5}$$

where the abbreviations

$$\boldsymbol{A}_e = \boldsymbol{A}_e^{11} - \boldsymbol{A}_e^{12}\,(\boldsymbol{A}_e^{22})^{-1}\,\boldsymbol{A}_e^{21} \quad \text{and} \quad \boldsymbol{a}_e \;= \boldsymbol{a}_e^1 - \boldsymbol{A}_e^{12}\,(\boldsymbol{A}_e^{22})^{-1}\,\boldsymbol{a}_e^2 \tag{6}$$

have been used. Having solved Equation (3) for $\Delta\hat{\boldsymbol{u}}_e$, the increments of the strains and stresses can be updated as follows

$$\begin{aligned} \Delta\boldsymbol{\alpha}_e^1 &= \boldsymbol{C}_e^{-1}\,(\boldsymbol{L}_e\,\Delta\hat{\boldsymbol{u}}_e + \boldsymbol{b}_e), \\ \Delta\boldsymbol{\alpha}_e^2 &= -(\boldsymbol{A}_e^{22})^{-1}\,(\boldsymbol{A}_e^{21}\,\Delta\boldsymbol{\alpha}_e^1 + \boldsymbol{a}_e^2), \\ \Delta\boldsymbol{\beta}_e &= \boldsymbol{C}_e^{-1}\,(\boldsymbol{A}_e\,\Delta\boldsymbol{\alpha}_e^1 + \boldsymbol{a}_e). \end{aligned} \tag{7}$$

The interested reader is referred to [3] or [2] for further details on element matrices and shape functions that have been neglected here for reasons of brevity.

2.2 | Modeling fibers and layers

Anisotropic material behavior is modeled as proposed in [4] using the simplified strain energy density function of the form

$$\begin{aligned} W = {} & k_1^{\text{iso}}(I_1-3)^2 + k_2^{\text{iso}}[(I_2-3)-2(I_1-3)] \\ & + k_1^{\text{ani}}(I_4-1)^2 + k_2^{\text{ani}}[(I_5-1)-2(I_4-1)] \\ & + k_c(I_1-3)(I_4-1), \end{aligned} \tag{8}$$

with the five material parameters $k_1^{\text{iso}}, k_2^{\text{iso}}, k_1^{\text{ani}}, k_2^{\text{ani}}$ and k_c, and the invariants of the right Cauchy-Green deformation tensor

$$I_1 = \operatorname{tr}(\mathbf{C}), \quad I_2 = \frac{1}{2}\left[\operatorname{tr}(\mathbf{C})^2 - \operatorname{tr}(\mathbf{C}^2)\right], \quad I_3 = \det\mathbf{C}, \quad I_4 = \operatorname{tr}(\mathbf{CM}), \quad I_5 = \operatorname{tr}(\mathbf{C}^2\mathbf{M}), \tag{9}$$

with the structural tensor $\mathbf{M} = \mathbf{n}\otimes\mathbf{n}$, where $\mathbf{n}$ denotes preferred fiber direction.

The second Piola-Kirchhoff stress tensor $\mathbf{S}^{\text{PK}}$, as well as the consistent tangent operator $\mathbb{C}$ can finally be obtained in classical fashion, viz.

$$\mathbf{S}^{\text{PK}} = \frac{\partial W}{\partial \mathbf{E}} = 2\frac{\partial W}{\partial \mathbf{C}} = 2\frac{\partial W}{\partial I_\alpha}\frac{\partial I_\alpha}{\partial \mathbf{C}}, \quad \mathbb{C} = 2\frac{\partial \mathbf{S}^{\text{PK}}}{\partial \mathbf{C}}, \quad \text{with} \quad \alpha = 1, \dots, 5. \tag{10}$$

3 | RESPONSE SENSITIVITY ANALYSIS

The method for the computation of sensitivity information is based on a variational approach as described in [2] in the context of geometric shape sensitivity analysis. This approach is founded on an enhanced kinematic viewpoint that offers a rigorous separation of geometric and physical effects within a deformation process. Choosing the direct way for sensitivity analysis, the sensitivity of the system response is derived as follows. The feasible design constraint says that a change in design must not violate the system's equilibrium, which leads to the vanishing total variation of the equilibrium condition, viz.

$$\delta R = \delta_u R + \delta_s R = k(\mathbf{v}, \delta\mathbf{u}) + p(\mathbf{v}, \delta\mathbf{s}) = 0, \tag{11}$$

with the stiffness operator

$$k(\mathbf{v}, \delta\mathbf{u}) = \frac{\partial R}{\partial \mathbf{u}}\delta\mathbf{u} \tag{12}$$

constituting the partial variation of the weak equilibrium w.r.t. the displacements, and the pseudoload operator

$$p(\mathbf{v}, \delta\mathbf{s}) = \frac{\partial R}{\partial \mathbf{s}}\delta\mathbf{s} \tag{13}$$

constituting the partial variation of the weak equilibrium w.r.t. design. In the work at hand, the design variables are chosen as the layer thicknesses and the fiber directions in each layer.

The discretized versions of the stiffness and pseudoload operators lead to the stiffness and pseudoload matrices

$$k^h(\boldsymbol{v}^h, \boldsymbol{u}^h) = \mathop{\mathsf{A}}_{e=1}^{\mathsf{nel}} \boldsymbol{v}_e^T \boldsymbol{K}_e \delta\boldsymbol{u}_e = \boldsymbol{v}^T \boldsymbol{K} \delta\boldsymbol{u}, \quad \text{with } \boldsymbol{K} \in \mathbb{R}^{\mathsf{n_u} \times \mathsf{n_u}} \tag{14}$$

and

$$p^h(\boldsymbol{v}^h, \boldsymbol{s}^h) = \mathop{\mathsf{A}}_{e=1}^{\mathsf{nel}} \boldsymbol{v}_e^T \boldsymbol{P}_e \delta\boldsymbol{s}_e = \boldsymbol{v}^T \boldsymbol{P} \delta\boldsymbol{s}, \quad \text{with } \boldsymbol{P} \in \mathbb{R}^{\mathsf{n_u} \times \mathsf{n_s}}, \tag{15}$$

where $\mathsf{n_u}$ and $\mathsf{n_s}$ denote the number of degrees of freedom and chosen design variables, respectively. Hence, excluding the trivial solution $\boldsymbol{v} = \boldsymbol{0}$, the discretized feasible design constraint can be rearranged so as to derive the total system's response sensitivity

$$\delta R^h = \boldsymbol{v}^T(\boldsymbol{K}\delta\boldsymbol{u} + \boldsymbol{P}\delta\boldsymbol{s}) = 0, \qquad \forall \boldsymbol{v} \in \mathbb{R}^{\mathsf{n_u}} \backslash \{\boldsymbol{0}\}, \quad \Leftrightarrow \quad \delta\boldsymbol{u} = -\boldsymbol{K}^{-1}\boldsymbol{P}\delta\boldsymbol{s} = \boldsymbol{S}\delta\boldsymbol{s}, \tag{16}$$

where $\boldsymbol{S}$ denotes the total response sensitivity matrix.

Within a structural optimization problem, the total gradient of any objective or constraint function of interest f can then easily be computed to

$$\delta f = \delta_u f + \delta_s f = \frac{\partial f}{\partial \boldsymbol{u}}\delta\boldsymbol{u} + \frac{\partial f}{\partial \boldsymbol{s}}\delta\boldsymbol{s} = \left(\frac{\partial f}{\partial \boldsymbol{s}} + \frac{\partial f}{\partial \boldsymbol{u}}\boldsymbol{S}\right)\delta\boldsymbol{s}. \tag{17}$$

4 | PRINCIPAL DESIGN INFLUENCES

The idea of design exploration is to use methods from PCA to identify design variables that have higher and lower impact on the structural response. In this work, SVD is used for this purpose. Briefly, the total response sensitivity that has been derived in the previous section represents the matrix form of the total derivative of the structural response w.r.t. changes in design, that is, $\boldsymbol{S} = \left[\frac{\mathrm{d}\boldsymbol{u}}{\mathrm{d}\boldsymbol{s}}\right]$. Interpreting this as an input-output system and applying SVD gives

$$\boldsymbol{S} \overset{\text{SVD}}{=} \Delta\hat{\boldsymbol{u}}\boldsymbol{W}\Delta\hat{\boldsymbol{s}}^T, \quad \text{with} \quad \Delta\hat{\boldsymbol{u}} \in \mathbb{R}^{\mathsf{n_u} \times \mathsf{n_u}}, \ \boldsymbol{W} \in \mathbb{R}^{\mathsf{n_u} \times \mathsf{n_s}}, \ \Delta\hat{\boldsymbol{s}}^T \in \mathbb{R}^{\mathsf{n_s} \times \mathsf{n_s}}, \tag{18}$$

where the left singular vectors are interpreted as changes in the structural response (output) and are therefore called response modes $\Delta\hat{\boldsymbol{u}}$, and the right singular vectors are interpreted as changes in design (input) and hence are called design modes $\Delta\hat{\boldsymbol{s}}$. $\boldsymbol{W}$ is a rectangular diagonal matrix and stores the singular values in decreasing order. These singular values are interpreted as weighting factors of the corresponding design mode, that is the higher the weighting factor, the higher the impact of the corresponding design mode on the structural response. A possible application of SVD is a low-rank approximation of the original matrix that still contains most of the information represented by the stored data. This is obtained by zeroing-out weighting factors (singular values) higher than a chosen rank R, viz.

$$\boldsymbol{S}^R = \begin{bmatrix} \Delta\hat{u}_1^1 & \Delta\hat{u}_1^2 & \dots & \Delta\hat{u}_1^{\mathsf{n_u}} \\ \vdots & \vdots & & \vdots \\ \Delta\hat{u}_{\mathsf{n_u}}^1 & \Delta\hat{u}_{\mathsf{n_u}}^2 & \dots & \Delta\hat{u}_{\mathsf{n_u}}^{\mathsf{n_u}} \end{bmatrix} \begin{bmatrix} W_1 & 0 & \dots & & 0 \\ 0 & W_2 & \dots & & 0 \\ \vdots & \vdots & \ddots & & \\ & & & W_R & \\ 0 & 0 & & & 0 \end{bmatrix} \begin{bmatrix} \Delta\hat{s}_1^1 & \Delta\hat{s}_1^2 & \dots & \Delta\hat{s}_1^{\mathsf{n_s}} \\ \vdots & \vdots & & \vdots \\ \Delta\hat{s}_{\mathsf{n_s}}^1 & \Delta\hat{s}_{\mathsf{n_s}}^2 & \dots & \Delta\hat{s}_{\mathsf{n_s}}^{\mathsf{n_s}} \end{bmatrix}^T. \tag{19}$$

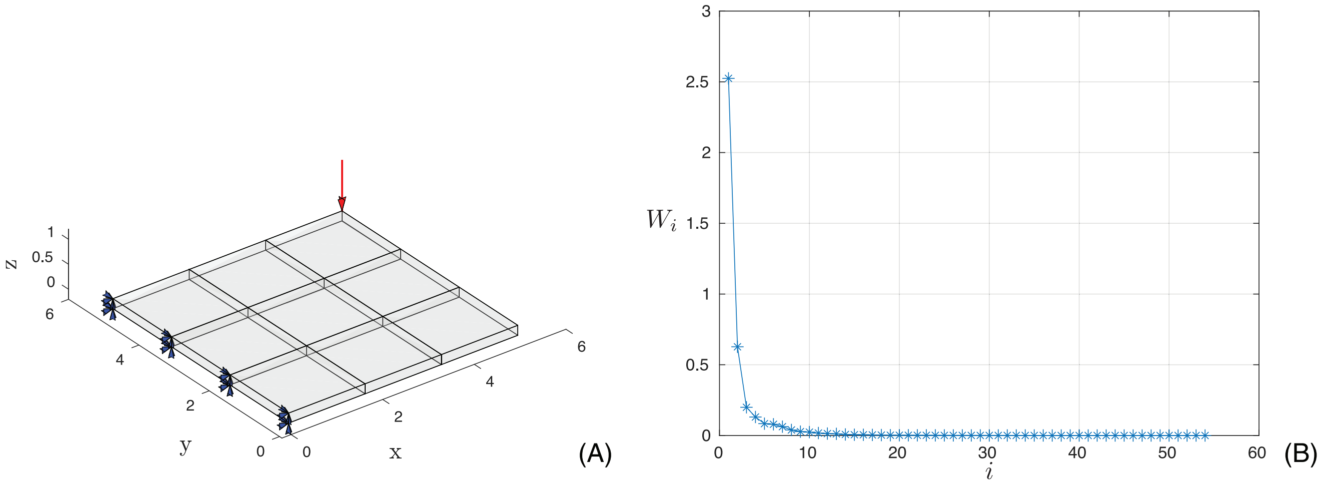

FIGURE 1 Academic example 1: (A) mechanical system, (B) singular values of corresponding response sensitivity matrix.

5 | ACADEMIC EXAMPLE

In this section small academic examples are chosen to stress the effectivity of SVD applied to sensitivity information in the context of model order reduction. Therefore, a 5 by 5 square plate is discretized using 9 solid-shell elements. Three layers with fiber angle orientations (90°|0°|90°) are chosen in thickness direction. Thus, in total $\mathsf{n}_{\mathsf{dv}} = 9 \cdot 2 \cdot 3 = 54$ design variables are chosen in the present examples. The set of material parameters is chosen as $k_1^{\mathsf{iso}} = 74.21$, $k_2^{\mathsf{iso}} = -99.45$, $k_1^{\mathsf{ani}} = -106.48$, $k_2^{\mathsf{ani}} = 298.35$, $k_c = 10.25$. In Figure 1A the mechanical system is illustrated, Figure 1B shows the singular values of the corresponding response sensitivity matrix of the system. Obviously, only a limited number of singular values significantly differ from zero, which gives rise to state that most of the sensitivity information can already be captured by a low-rank approximation of the corresponding sensitivity data.

In Figure 2 heatmap plots of the original (A) and a rank-1 approximation (B) of the response sensitivity matrix are given. The rows represent the components of the structural response, while the columns represent the design variables. Note that the pictured values are absolute and normalized so as to be better comparable. In the first 27 columns, that is, in the first half, the sensitivity w.r.t. the layer thicknesses are pictured and in the latter 27 columns, the sensitivity w.r.t. the fiber angles are pictured. The brighter (more red) the pixel, the higher the impact of the corresponding design variable on the structural response.

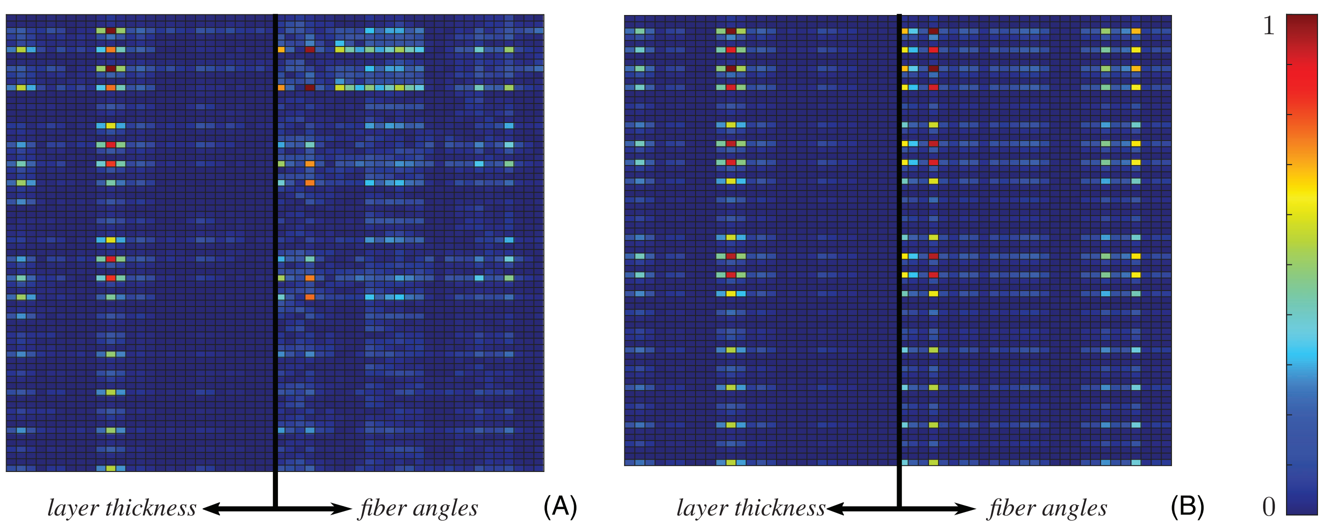

FIGURE 2 Heatmap of response sensitivity matrices: (A) original, (B) rank-1 approximation.

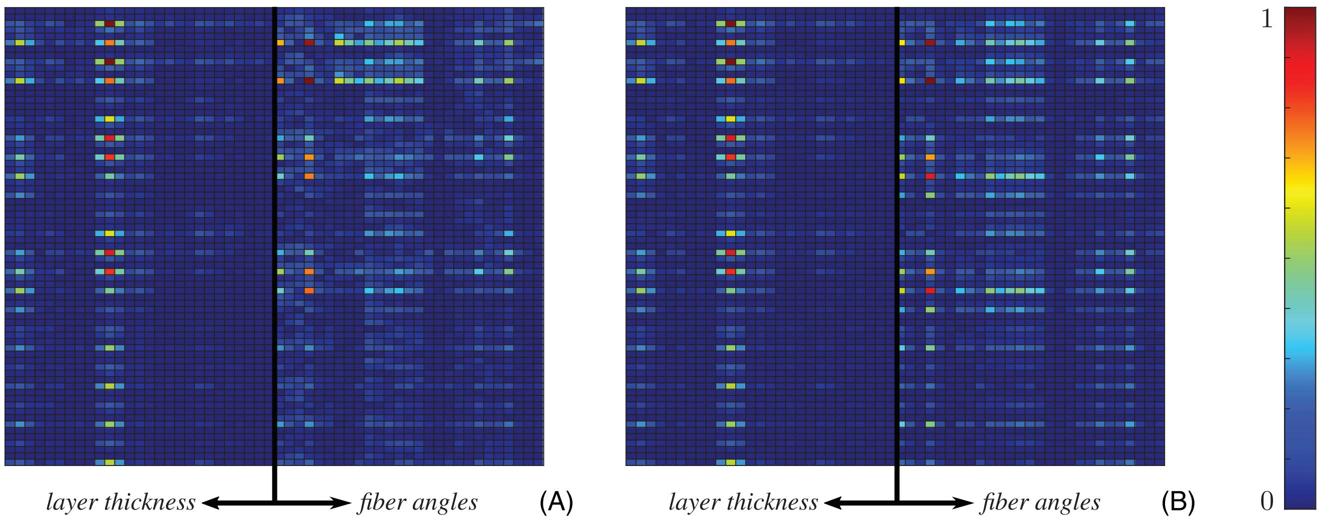

FIGURE 3 Heatmap of response sensitivity matrices: (A) original, (B) rank-3 approximation.

It is clearly observable that even with a rank-1 approximation most of the influencing design variables are already detected. This effect becomes even more obvious by choosing more weighting factors (singular values), that is, approximate the response sensitivity matrix with slightly higher rank, as can easily be observed in Figure 3.

For comparison, a second academic example is chosen, as shown in Figure 4, in which only the Dirichlet and Neumann boundary conditions have been changed compared to the previous example. As can be observed from Figure 5 and Figure 6, to capture most of the important design parameters, a higher rank approximation is necessary, especially in case of the fiber angles as can clearly be seen of Figure 6B, where the second half of the rank-4 approximation still apparently differs from the original.

6 | CONCLUSIONS AND DISCUSSIONS

The presented methodology of sensitivity based design exploration for layered composite shells using SVD has demonstrated its effectiveness in compressing meaningful sensitivity information and potential in detecting major design modes with high impact on structural response for optimizing the structural performance. This can for example be utilized by transformation of the considered optimization problem into lower dimensional space spanned by chosen orthonormal design modes (right singular vectors). For this, the change in design is parameterized by scaling factors $\boldsymbol{\omega} \in \mathbb{R}^{n_m}$ weighting

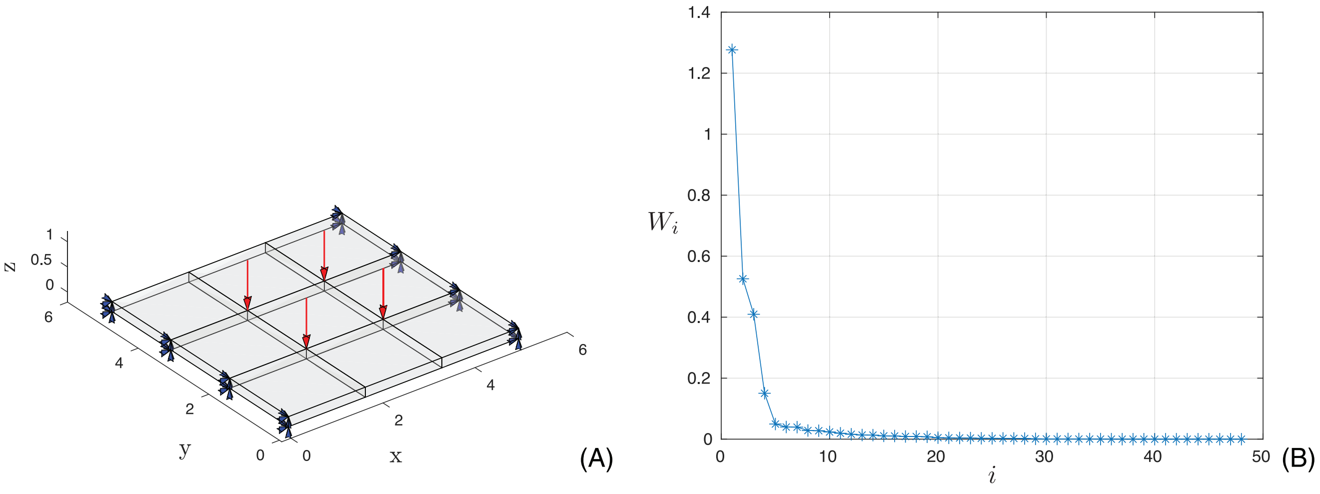

FIGURE 4 Academic example 2: (A) mechanical system, (B) singular values of corresponding response sensitivity matrix.

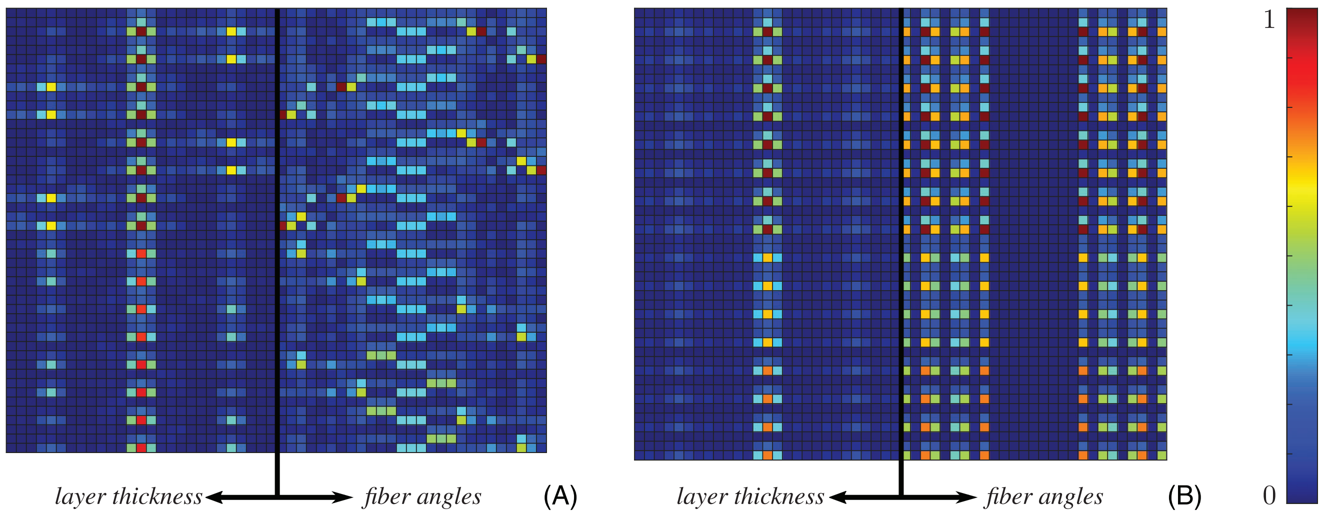

FIGURE 5 Heatmap of response sensitivity matrices: (A) original, (B) rank-1 approximation.

the n_m chosen design modes

$$\Delta\bar{\boldsymbol{s}} := \omega_1 \Delta\hat{\boldsymbol{s}}_1 + \omega_2 \Delta\hat{\boldsymbol{s}}_2 + \cdots + \omega_{n_m} \Delta\hat{\boldsymbol{s}}_{n_m} \tag{20}$$

and the gradient of any objective or constraint function $f(\bar{\boldsymbol{s}})$ w.r.t. the scaling factors can be computed to

$$\delta f = \frac{\partial f}{\partial \bar{\boldsymbol{s}}} \frac{\mathrm{d}\bar{\boldsymbol{s}}}{\mathrm{d}\boldsymbol{\omega}} \delta\boldsymbol{\omega}, \quad \text{with} \quad \frac{\mathrm{d}\bar{\boldsymbol{s}}}{\mathrm{d}\boldsymbol{\omega}} = \begin{bmatrix} \Delta\hat{\boldsymbol{s}}_1 & \Delta\hat{\boldsymbol{s}}_2 & \dots & \Delta\hat{\boldsymbol{s}}_{n_m} \end{bmatrix} \in \mathbb{R}^{n_s \times n_m}. \tag{21}$$

Comparison of the low-rank approximations of any important gradient information, as shown in the examples in Section 5, can then for instance be used to define a mode selection criterion. However, several open questions remain regarding the generality and validity of the method for real-world optimization problems and its applicability to different engineering applications.

Firstly, in order to establish the practical relevance of the proposed method, it is crucial to validate its effectiveness in real-world optimization examples. While the theoretical foundation and preliminary results are promising, the applicability of SVD-based design exploration to complex composite structures encountered in engineering practice needs further investigation. Real-world optimization examples involving layered composite shells from aerospace, automotive,

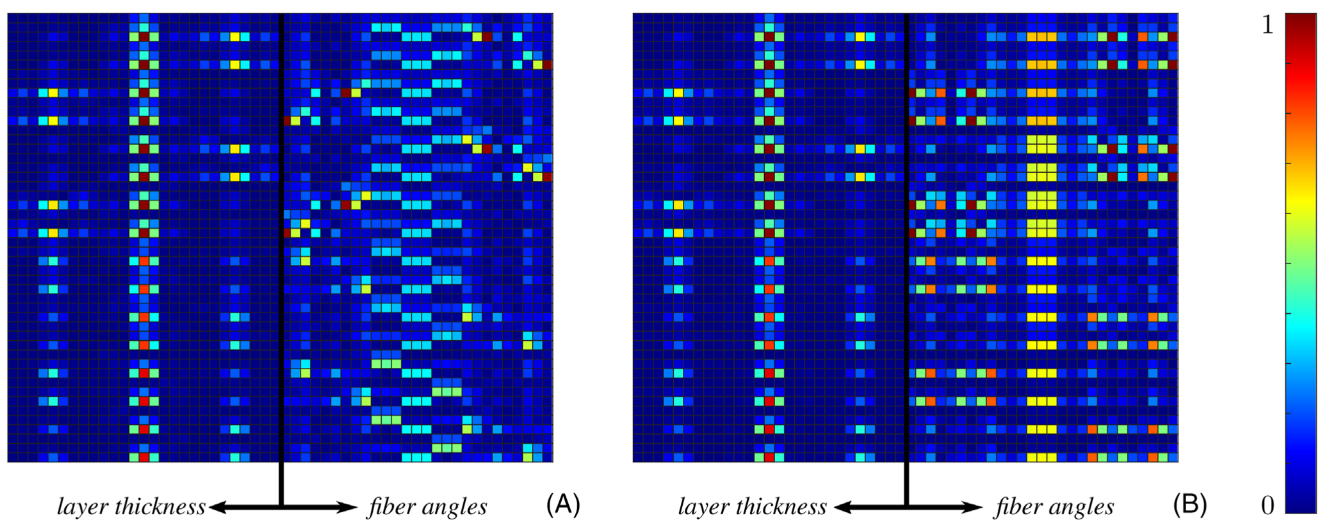

FIGURE 6 Heatmap of response sensitivity matrices: (A) original, (B) rank-4 approximation.

and civil engineering applications should be studied to assess the method's performance and validate its effectiveness in achieving improved designs. Such validation studies will enhance confidence in the applicability of the method to real-world scenarios.

Secondly, the potential applications of the SVD-based design exploration method extend beyond layered composite shells. The method can be adapted and applied to various engineering fields, including but not necessarily limited to structural engineering, mechanical engineering, materials science, and biomedical engineering. By customizing the methodology suiting the specific characteristics of different applications, it becomes possible to explore the design space and identify critical parameters in various engineering disciplines. Investigating and documenting the successful application of the presented method to different contexts will provide valuable insights and expand its practical utility.

In conclusion, while the design exploration method based on SVD shows promise for fiber reinforced composite shells, further research is needed to address the open questions discussed. Validating the method through real-world optimization examples and exploring its application in various engineering areas will contribute to its practical applicability and efficiency. By addressing these questions, the SVD-based design exploration can evolve into a valuable tool for optimizing fiber reinforced composite structures and enhancing their performance in a wide range of engineering applications.

ACKNOWLEDGMENTS

This work is part of the DFG project *Combined shape and cross section optimization of fiber reinforced structures based on singular value decomposition of sensitivity information* that is funded by the Deutsche Forschungsgemeinschaft (DFG), which is gratefully acknowledged by the authors.

Open access funding enabled and organized by Projekt DEAL.

ORCID

Jan Liedmann https://orcid.org/0000-0001-8759-6940

REFERENCES

1. Jia, W., Sun, M., Lian, J., & Hou, S. (2022). Feature dimensionality reduction: A review. *Complex & Intelligent Systems*, *8*, 2663–2693.
2. Gerzen, N., Barthold, F. J., Klinkel, S., Wagner, W., & Materna, D. (2013). Variational sensitivity analysis of a non-linear solid shell element. *International Journal for Numerical Methods in Engineering*, *96*(1), 29–42.
3. Klinkel, S., Gruttmann, F., & Wagner, W. (1999). A continuum based three-dimensional shell element for laminated structures. *Computers and Structures*, *71*, 43–62.
4. Barfusz, O., Smeenk, R., & Reese, S. (2018). *Solid-Shells based on reduced integration - Geometrically non-linear analysis of layered structures*. ECCM6 / ECFD 7 Glasgow.

How to cite this article: Liedmann, J., Barthold, F.-J., & Gerzen, N. (2023). Gradient-based determination of principal design influences on composite structures. *Proceedings in Applied Mathematics and Mechanics*, *23,* e202300177. https://doi.org/10.1002/pamm.202300177